JACS
JOURNAL OF THE AMERICAN CHEMICAL SOCIETY

COMMUNICATION

pubs.acs.org/JACS

Synthesis of Colloidal HgTe Quantum Dots for Narrow Mid-IR Emission and Detection

Sean Keuleyan, Emmanuel Lhuillier, and Philippe Guyot-Sionnest*

The James Franck Institute at the University of Chicago, 929 East 57th Street, Chicago, Illinois 60637, United States

Supporting Information

ABSTRACT: HgTe colloidal quantum dots are prepared via a simple two-step injection method. Absorption and photodetection with sharp edges, as well as narrow photoluminescence, are tunable across the near and mid-IR between 1.3 and 5 μm.

In the past decade, colloidal quantum dots (CQDs) have been explored for many optoelectronic applications.[1,2] The common Zn and Cd based CQDs cover the UV and visible spectra.[3] Tunability across the near-infrared (near-IR) has been achieved with the lead chalcogenides, reaching wavelengths up to 4 μm with PbSe.[4] Among the possible materials that may cover the mid-infrared (mid-IR) as CQDs, the semimetal HgTe can, in principle, cover the full range by simply tuning the size.[5] We recently reported that HgTe CQDs afford photocurrent detection in the first mid-IR atmospheric transparency range (3−5 μm),[6] promising a low-cost alternative to established infrared materials.[7]

The mercury chalcogenide CQDs had been studied for some time. HgTe CQDs were first synthesized in aqueous reactions and showed broad absorption and PL in the visible and near-IR.[8−10] Relatively narrow absorption and PL from small particles of HgS and $HgSe_{1-x}S_x$ were achieved at visible wavelengths by controlling reactivity through a phase separation.[11,12] Kovalenko et al. prepared small HgTe particles active in the near-IR with fairly narrow spectral features.[13] Particles of diameter larger than 4 nm then required a postsynthetic heat-induced Ostwald ripening. This gave particles of up to 10 nm diameters with absorption up to 3 μm and PL to 3.5 μm, but broadened the size distributions. In our prior work, we reacted mercury salts and trialkylphosphine tellurium precursors, in ethanol or butanol with coordinating amines.[6] The transport properties were suitable for photocurrent detection but the spectral features for sizes above 10 nm were broad. Future mid-IR devices will benefit from the synthesis of HgTe CQDs with improved monodispersivity.

To obtain controlled growth at rather large sizes in an organic solvent, the particles should have a good surface passivation by long chain ligands for stabilization against van der Waals forces and slow particle diffusion to limit aggregation. In addition, HgTe needs to be synthesized at low temperatures to avoid uncontrolled growth to bulk sizes. This led us to the method developed by Cademartiri et al. for the synthesis of PbS nanoparticles.[14] They showed that, at high concentrations (molar ratio 1:2), $PbCl_2$ in oleylamine is a viscous mixture, and that injection of S dissolved in oleylamine at 80 °C maintains good size distribution over long growth times. Moreels et al. expanded this preparation to cover a larger spectral range using TOP.[15]

Primary amines are similarly weak ligands for Hg(II) but can easily dissolve mercury(II) chloride. Therefore, $HgCl_2$ is first dissolved with a long chain amine such as oleylamine at 100 °C for about 1 h under vacuum and then placed under Ar and cooled to 80 °C. $HgCl_2$ and oleylamine form a viscous mixture at high concentration; however, we found optimal growth to occur at Hg/oleylamine ratios of about 1:120 where it is still a fluid solution. A solution of Te in tri-*n*-octylphosphine (TOPTe) is then rapidly injected. On addition of the TOPTe, the solution darkens, appearing black after roughly 15−30 s, and the growth is monitored by extractions to a quench solution of long chain thiols in C_2Cl_4. The particle size is controlled by the injection temperature and the duration of the reaction, with the smallest particles obtained at 60 °C, and the largest above 100 °C. The reaction is believed to occur through the mechanism described by Howes et al., where the Hg(II) chloride is reduced by the TOPTe, in this case forming HgTe and the trioctylphosphine dichloride.[16,17] The narrow size distribution enables the full product solution to be used in spectroscopic studies without any size selection. Method details and the evolution of the photoluminescence (PL) peak position during the reaction at different temperatures are provided in the Supporting Information.

The optical properties of this material are significantly better defined than in previous reports on mercury chalcogenides. A series of absorption spectra for samples of different sizes are shown in Figure 1a, where larger particles give an absorption onset at lower frequencies. The first excitonic peak is observed in all spectra and tunes from 1.5 to close to 5 μm. A second feature is also seen at shorter wavelengths. The absorption edge is much sharper than previously, rising from 10 to 90% absorption in typically less than 500 cm^{-1} width. The PL is narrower as well with full width at half-maximum often less than 500 cm^{-1}. Typical PL spectra are shown in Figure 1b. The Stokes shift is small, which is a further indication of the sample narrow size dispersion (Supplementary Figure 2).

Transmission electron microscopy (TEM) images and X-ray diffraction (XRD) data are shown in Figure 2. The diffraction data shows distinct peaks corresponding to zinc-blende (ZB) HgTe. The particles often appear as triangles or distorted parallelograms, which is consistent with approximately tetrahedral shapes. A tetrahedral shape would naturally arise for ZB nanocrystals when the temperature is low enough that the growth rates are different on the various

Received: August 22, 2011
Published: September 25, 2011

dx.doi.org/10.1021/ja2079509 | *J. Am. Chem. Soc.* 2011, 133, 16422–16424

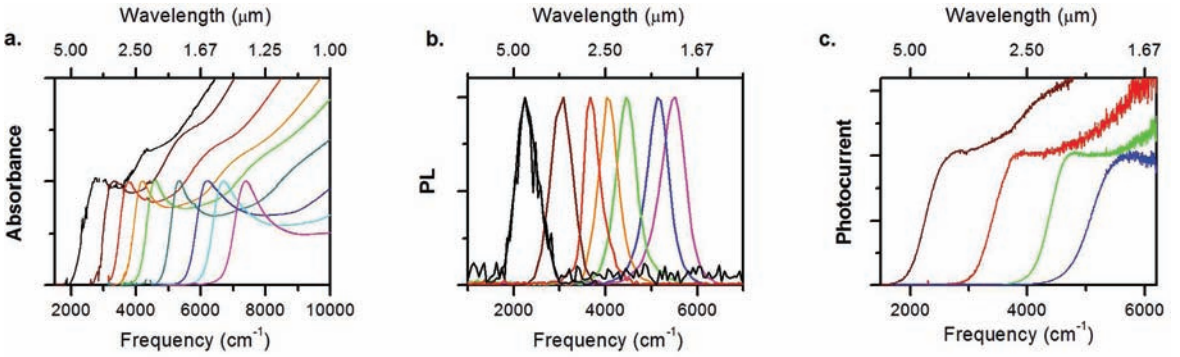

Figure 1. Normalized spectra. (a) Absorption of solutions of HgTe CQDs in C_2Cl_4. The C−H absorbance from the ligands has been subtracted for clarity. (b) Photoluminescence of HgTe CQDs in C_2Cl_4. (c) Photoconduction spectra of films of colloidal HgTe nanoparticles of different sizes. The films have typical OD ∼ 0.1 at the exciton and are roughly 100 nm thick.

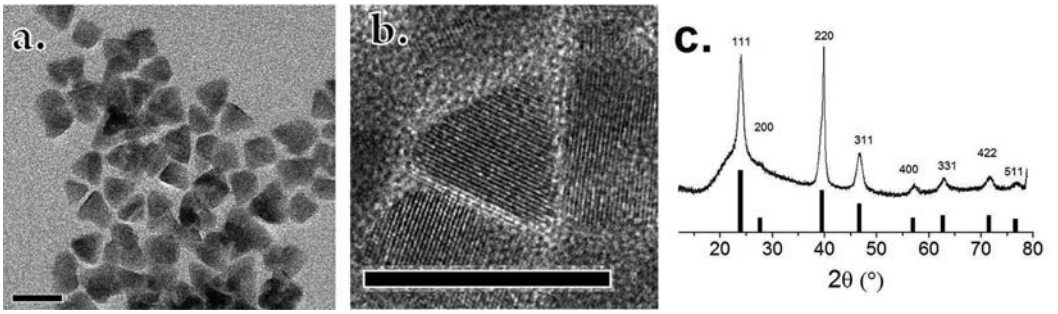

Figure 2. (a) TEM image of HgTe nanoparticles having a PL peak near 2460 cm^{-1} (0.305 eV). (b) HRTEM image showing interplanar spacing of 0.37 nm in a single particle. Scale bars are 20 nm. (c) XRD spectrum with labeled bulk HgTe diffraction angles.[18].

facets. The sample shown in Figure 2 has a mean edge length of approximately 14.5 nm, defined as the length of the edge of the triangular shape, and has a PL peak position of 2460 cm^{-1} (0.305 eV). The triangular particles often display lattice spacing of 0.37 nm, consistent with the separation between {111} planes with a 6.46 Å lattice constant for ZB HgTe.[19] The observed shapes and the frequently observed {111} fringes for the triangles could suggest a tetrahedral shape, possibly truncated, resting on a {112} plane.

Films were prepared by drop-casting solutions of colloidal HgTe QDs on interdigitated electrodes.[6] In contrast to the previous results with the partially aggregated HgTe dots,[6] the drop-cast films were highly insulating, with dark resistivities typically >10^{10} Ohm cm^{-1}. Ligand exchange within the films readily improves the conductivity by reducing the barrier width between particles.[20] With ligand exchange to ethanedithiol, the room temperature dark resistivity decreased to ∼10^{3-5} Ω cm^{-1}. With such films made with solutions of different particle sizes, the photocurrent spectral response was easily measured with a standard Fourier Transform Infrared Spectrometer. Photoresponse spectra are shown in Figure 1c for several samples, which cover the mid-IR range. Compared to previous results, the sharper onset will be advantageous in multicolor devices.

In summary, a new synthesis of HgTe colloidal quantum dots has been developed to produce spectrally monodisperse particles in high yield. The material covers the first mid-IR atmospheric transparency window from 3 to 5 μm, with well-defined absorption edges. It also shows the reddest room temperature photoluminescence and photoconductance reported to date with CQDs. This new material will lead to further advances in applying colloidal quantum dot materials for mid-IR applications.

■ ASSOCIATED CONTENT

Ⓢ Supporting Information. Method and measurement details, additional spectra, the evolution of the PL peak position as a function of reaction time at different temperatures, and a TEM size measurement histogram. This material is available free of charge via the Internet at http://pubs.acs.org.

■ AUTHOR INFORMATION

Corresponding Author
pgs@uchicago.edu

■ ACKNOWLEDGMENT

This work was supported by the DARPA COMPASS program through a grant from ARO.

■ REFERENCES

(1) Konstantatos, G.; Sargent, E. H. *Nat. Nanotechnol.* **2010**, *5*, 391–400.
(2) Talapin, D.; Lee, J.; Kovalenko, M.; Shevchenko, E. *Chem. Rev.* **2010**, *110*, 389–458.
(3) Klimov, V. I., Ed.; *Nanocrystal Quantum Dots*, 2nd ed.; Taylor and Francis: Boca Raton, Fl, 2009.

(4) Pietryga, J.; M. Schaller, R. D.; Werder, D.; Stewart, M. H.; Klimov, V. I.; Hollingsworth, J. A. *J. Am. Chem. Soc.* **2004**, *126*, 11752–11753.
(5) Rogach, A. L.; Eychmüller, A.; Hickey, S. G.; Kershaw, S. V. *Small* **2007**, *3*, 536–557.
(6) Keuleyan, S.; Lhuillier, E.; Brajuskovic, V.; Guyot-Sionnest, P. *Nat. Photonics* **2011**, *5*, 489–493.
(7) Rogalski, A.; Antoszewski, J.; Faraone, L. *J. Appl. Phys.* **2009**, *105*, 091101.
(8) Rogach, A.; Kershaw, S.; Burt, M.; Harrison, M.; Kornowski, A.; Eychmuller, A.; Weller, H. *Adv. Mater.* **1999**, *11*, 552–555.
(9) Rogach, A.; Harrison, M.; Kershaw, S.; Kornowski, A.; Burt, M.; Eychmuller, A.; Weller, H. *Phys. Status Solidi B* **2001**, *224*, 153–158.
(10) Harrison, M.; Kershaw, S.; Rogach, A.; Kornowski, A.; Eychmuller, A.; Weller, H. *Adv. Mater.* **2000**, *12*, 123–125.
(11) Higginson, K.; A. Kuno, M.; Bonevich, J.; Qadri, S.; B. Yousuf, M.; Mattoussi, H. *J. Phys. Chem. B* **2002**, *106*, 9982–9985.
(12) Kuno, M.; Higginson, K. A.; Qadri, S. B.; Yousuf, M.; Lee, S. H.; Davis, B. L.; Mattoussi, H. *J. Phys. Chem. B* **2003**, *107*, 5758–5767.
(13) Kovalenko, M. V.; Kaufmann, E.; Pachinger, D.; Roither, J.; Huber, M.; Stangl, J.; Hesser, G.; Schaffler, F.; Heiss, W. *J. Am. Chem. Soc.* **2006**, *128*, 3516–3517.
(14) Cademartiri, L.; Bertolotti, J.; Sapienza, R.; Wiersma, D. S.; von Freymann, G.; Ozin, G. A. *J. Phys. Chem. B* **2006**, *110*, 671–673.
(15) Moreels, I.; Justo, Y.; De Geyter, B.; Haustraete, K.; Martins, J. C.; Hens, Z. *ACS Nanotechnol.* **2011**, *5*, 2004–2012.
(16) Howes, P.; Green, M.; Johnston, C.; Crossley, A. *J. Mater. Chem.* **2008**, *18*, 3474–3480.
(17) Godfrey, S. M.; McAuliffe, C. A.; Pritchard, R. G.; Sheffield, J. M.; Thompson, G. M. *J. Chem. Soc., Dalton Trans.* **1997**, 4823–4828.
(18) Gong, P., ICDD Grant-in-Aid; Polytechnic Institute of New York: Brooklyn, New York, 1981.
(19) Chu, J.; *HgTe: Lattice Parameter*; Roessler, U., Ed.; SpringerMaterials - The Landolt-Börnstein Database (http://www.springermaterials.com); Springer-Verlag: Berlin Heidelberg, 2008. DOI: 10.1007/978-3-540-74392-7_117.
(20) Yu, D.; Wang, C.; Guyot-Sionnest, P. *Science* **2003**, *300*, 1277–1280.